Journal of Hazardous Materials 436 (2022) 128995

Contents lists available at ScienceDirect

Journal of Hazardous Materials

journal homepage: www.elsevier.com/locate/jhazmat

Research Paper

Rapid sequestration of perovskite solar cell-derived lead in soil

Felix Schmidt [a,b], Luca Ledermann [a], Andreas Schäffer [b], Henry J. Snaith [c], Markus Lenz [a,d,*]

[a] Institute for Ecopreneurship, School of Life Sciences, University of Applied Sciences and Arts Northwestern Switzerland, Hofackerstrasse 30, 4132 Muttenz, Switzerland
[b] Institute for Environmental Research, RWTH Aachen University, Worringerweg 1, 52074 Aachen, Germany
[c] Department of Physics, University of Oxford, Clarendon Laboratory, Parks Road, Oxford OX1 3PU, UK
[d] Sub-Department of Environmental Technology, Wageningen University, 6700 AA Wageningen, The Netherlands

HIGHLIGHTS

- Availability of perovskite derived Pb is rapidly decreased and naturally limited in soils.
- The fate of perovskite derived Pb was not different from that of other Pb sources.
- Only in extreme scenarios, perovskite derived Pb may have a negative impact on soils.

GRAPHICAL ABSTRACT

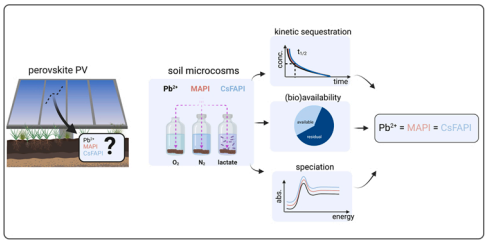

ARTICLE INFO

Edited by: Lingxin Chen

Keywords:
Perovskite solar cells
Environmental impact
Sequential extraction
Environmental fate
XANES
Lead sequestration

ABSTRACT

Efficient and stable perovskite solar cells rely on the use of Pb species potentially challenging the technologies' commercialisation. In this study, the fate of Pb derived from two common perovskite precursors is compared to cationic lead in soil-water microcosm experiments under various biogeochemical conditions. The rapid and efficient removal of Pb from the aqueous phase is demonstrated by inductively coupled plasma mass spectrometry. Sequential soil extraction results reveal that a substantial amount of Pb is associated with immobile fractions, whereas a minor proportion of Pb may become available again in the long term, when oxygen is depleted (e.g. during water logging). X-ray absorption spectroscopy results reveal that the sorption of Pb on mineral phases represents the most likely sequestration mechanism. The obtained results suggest that the availability of leached Pb from perovskite solar cells is naturally limited in soils and that its adverse effects on soil biota are possibly negligible in oxic soils. All three Pb sources used behaved very similar in the experiments, wherefore we conclude that perovskite derived Pb will have a similar fate compared to cationic Pb, so that established risk assessment considerations for Pb remain legitimate.

1. Introduction

Perovskite solar cells (PSCs) have been a success story in scientific research (Kojima et al., 2009; Lee et al., 2012; Grätzel, 2017). A decade after their discovery, the efficiency of lab-scale PSC devices has surpassed that of conventional thin-film photovoltaics (PV), such as cadmium telluride (CdTe) or copper-indium-gallium selenide (Green et al., 2019). The market leader, silicon-based PV, has been challenged regarding single-junction solar cell efficiency. Tandem-approaches enable further efficiency enhancement and cost minimisation and thus

* Corresponding author at: Institute for Ecopreneurship, School of Life Sciences, University of Applied Sciences and Arts Northwestern Switzerland, Hofackerstrasse 30, 4132 Muttenz, Switzerland.
E-mail address: markus.lenz@fhnw.ch (M. Lenz).

https://doi.org/10.1016/j.jhazmat.2022.128995
Received 23 February 2022; Received in revised form 16 April 2022; Accepted 20 April 2022
Available online 25 April 2022

have paved a potential way to overcome silicon's soon-to-be-faced fundamental performance limitations (Case et al., 2019). Extensive research has been undertaken to improve the stability of PSCs, which is currently considered to be one of the key challenges to enable market entry (Rong et al., 2018; Liu et al., 2019). Intrinsic instability under various environmental stressors (such as heat, moisture, UV light and biofilm formation) and degradation processes are also actively tackled (Urbina, 2020; Habisreutinger et al., 2016).

However, PSCs also pose an intrinsic environmental threat due to their reliance upon the use of lead salts in their crystal structure (Babayigit et al., 2016; Hailegnaw et al., 2015; Li et al., 2020). The absorber material crucially relies on the use of Pb in concentrations on the order of 0.5 g/m^2 (Fabini, 2015). Pb-free PSCs do not exhibit the stability and efficiency of their Pb-based counterparts (Ke and Kanatzidis, 2019; Kamat et al., 2017). For example, Sn^{2+}-based PSCs have rarely exceeded a 10-% power-conversion efficiency on the lab-scale and are more prone to degradation due to Sn^{2+} oxidation (Jokar et al., 2019; Diau et al., 2019; Nishimura et al., 2020). Thus, Pb-based PSCs likely remain the only viable option due to their high stability and efficiency.

Pb^{2+} may be emitted into the environment during the use phase, if PSCs are physically damaged as well as upon the end-of-life, if PSCs are inappropriately disposed of. Lead halides are the main degradation products after perovskite hydrolysis, and they are well to sparingly soluble in water [$K_{sp}(PbI_2) = 4.41 \times 10^{-9}$ M]. In contrast, Cd-based species (from CdTe PV) are highly insoluble, with solubility products 15–20 orders of magnitude less than those of lead halides (Fthenakis et al., 2020). Pb^{2+} does not have any known physiological role in biota and exerts adverse effects at low concentrations. For example, the US Environmental Protection Agency has set a threshold value of only 15 μg/L for Pb^{2+} in drinking water.

Pb^{2+} cannot be considered to be a new contaminant (Bell, 1924; Chaney et al., 1989; Ata et al., 2019). Early applications in gasoline, leaching from old water pipes and fracking processes have resulted in Pb^{2+} contamination world-wide (Bellinger, 2016; Taylor et al., 2016). Regarding PSCs, a majority of studies have tackled this issue from a life-cycle assessment perspective (Celik et al., 2016; Espinosa et al., 2015). Some initial laboratory studies concerning the potential fate of PSC-derived Pb in the environment have been reported. Hailegnaw et al. have reported the rapid and quantitative leaching of Pb through rain impact (Hailegnaw et al., 2015). Yoo et al. (2019) have demonstrated that PbI_2 and PbO – supposed degradation products of PSCs after hydrolysis and combustion in case of fire – would be considerably sorbed on soils, mitigating the risk of Pb^{2+} mobility. However, the tested concentrations were high (above the solubility products of the spiked Pb model species); hence, the sorption potential may have been overestimated due to limited water solubility and needs to be elucidated at a sufficiently low Pb concentration. The kinetics of Pb sequestration are key to assessing whether PSCs represent an environmental risk, because the kinetics determine the concentration and exposure time of soil organisms to the metal. The sequestration mechanism determines susceptibility to long-term re-mobilisation, when the soil biogeochemical conditions change as a result of anthropogenic processes (such as soil compaction, irrigation, construction works) or natural processes (periodic flooding, heavy rainfall, microbial activity).

Therefore, here we investigate the extent to which and how quickly various perovskite-derived Pb species are removed from aqueous solution in contrasting biogeochemical conditions (including aerobic, anaerobic, and with stimulated microbial activity) using soil-rainwater microcosms. Aqueous metal concentrations were determined by triple quadrupole inductively coupled plasma mass spectrometry (QqQ-ICP-MS), and the dissipation half-life of aqueous Pb was derived. Thermodynamic equilibrium modelling and sequential extraction were employed to examine the foreseen mobility of Pb (immediate and medium-term, respectively), while X-ray absorption near edge structure (XANES) spectroscopy was used to elucidate the sorption mechanism of sequestered Pb in soil.

2. Materials and methods

2.1. Soil source

The soil originated from Eiken (Switzerland) and had been fully characterised previously (Evangelou et al., 2014). In brief, the soil was a loamy sand (77% sand, 13% loam, and 10% clay) subsoil with 1.5% organic matter, 0.16% $CaCO_3$ content and maximal water holding capacity of 40% (Evangelou et al., 2014). The Pb background Pb concentration was low and determined to be 17 ± 1 mg/kg via microwave-assisted acid digestion (MARS 6, CEM GmbH, Kamp-Lintfort, Germany) (Table S1, Supporting Information). It was stored in the dark at room temperature until use.

2.2. Chemicals and reagents

If not specified otherwise, chemicals were purchased from commercial sources (Sigma-Aldrich, Buchs, Switzerland; Merck, Zug, Switzerland) at a high purity (> 99%) and used without further purification. Synthetic rainwater (Smith et al., 2002) was prepared with the following composition (mg L^{-1}): NaCl (4.3); $MgCl_2{\cdot}7H_2O$ (7.3), $CaCl_2{\cdot}6H_2O$ (6.1), KCl (0.7), $NaNO_3$ (3.1) and Na_2SO_4 (6.0), with a pH of 7.1. Three Pb-based materials were used in the assessment. These were a highly soluble lead salt, $Pb(NO_3)_2$, and two precursor sets for perovskite materials (methylammonium lead triiodide, ($CH_3NH_3PbI_3$, MAPI) and caesium-formamidinium lead triiodide ($Cs_{0.17}(NH_2CH=NH_2)_{0.83})PbI_3$, CsFAPI)). The salts (TCI Chemicals, Tokyo, Japan) were pre-diluted in synthetic rainwater, followed by sonication for 10 min and subsequent spiking into the microcosms.

2.3. Microcosm setup

Five-gram aliquots of the soil were added into 50 mL serum bottles and spiked with Pb species to achieve a final concentration of 100 mg Pb/kg soil and a soil:water ratio of 1:5 (m/v). This addition corresponded to a 5.9-fold increase in the Pb system concentration relative to background concentrations and equated to a completely leached PSC area of 9.9 cm^2 being spiked into this miniaturised system (assuming 420 mg Pb/m^2 PSC) (Fabini, 2015).

Aerobic microcosms were kept open to the atmosphere, while anaerobic microcosms were purged with N_2 for 30 min using a custom automatic gas-exchange system and sealed with a butyl stopper and crimp seal prior to spiking. Microbial activity was stimulated in one set of the sealed microcosms by the addition of lactate as a sodium-(DL)-lactate solution (15 mM). Soil-free microcosms were used as a positive control to account for potential evaporation during incubation time. Background Pb levels were monitored using unspiked systems. All conditions were tested in triplicate and placed on a rotational shaker (Edmund Bühler KS-10 Shaker, 5 rcf). Solution pH and redox potential were monitored using a Metrohm 713 pH metre equipped with a pH electrode or a Pt redox electrode, and where applicable, under inert conditions (GC Glovebox Systemtechnik GmbH, < 10 ppm O_2).

2.4. Aqueous Pb determination

Total Pb concentration of the aqueous phase was monitored during the initial 24 h of the experiments. For this, 500 μL aliquots were sampled at a depth of approx. 1 cm, filtered (0.45 μm syringe filter; WICOM International AG, Chur, Switzerland), diluted in 3% HNO_3 (semiconductor grade) using an autodilution system (Simprep, Teledyne Cetac Technologies, USA). Samples were then analysed by QqQ-ICP-MS. Analysis was performed on an 8800 QqQ-ICP-MS system (Agilent, Basel, Switzerland) using general-purpose operational settings. Lead was quantified as $^{208}Pb^+$ using helium collision gas (5 mL/min). Quantification was carried out using an external calibration from a single-element standard prepared in milliQ water (18.2 MΩ/cm, Arium Pro,

Sartorius GmbH, Göttingen, Germany) from 0 to 50 μg/L and was considered appropriate if $R^2 > 0.9995$. $^{103}Rh^+$ was monitored as an internal standard. The Pb concentration measured over time was fitted using a four-parameter logistic regression in GraphPad Prism 8 with constraints on normalisation between 0% and 100%, and the dissipation half-life (i.e., the time required for the aqueous Pb concentration to be reduced to half of its initial value) was derived (Table S2, Supporting Information).

2.5. Sequential extraction

The foreseen mobility of Pb in microcosms was evaluated after short-term (48 h) and medium-term (16 d) exposure by a sequential extraction scheme (Quevauviller, 2002). Briefly, the wet soil was treated with increasingly harsh chemicals, and the resulting Pb concentration of the supernatant was measured by QqQ-ICP-MS (Table S3, Supporting Information). To do so, the microcosm was sacrificed and transferred into a 50 mL polypropylene tube. The suspension was then centrifuged (12 min, 4700 relative centrifugal force, centrifuge 5804R, Eppendorf, Schönenbuch, Switzerland), the supernatant was discarded and residual soil was washed with 20 mL of water. After discarding the aqueous supernatant, a sonication-assisted, accelerated sequential extraction was carried out (Table S3, Supporting Information) (Quevauviller, 2002; Arain et al., 2008). The accelerated sequential extraction was validated based on BCR-701 reference material (Fig. S1, Supporting Information). The accelerated, sequential extraction showed quantitative Pb recovery (107 ± 7%) across all reactors. The amount of Pb extracted in step 1 + 2 ('exchangeable' and 'reducible') may be prone to mobilisation (either by ion exchange or upon reductive dissolution of soil Mn/Fe phases), whereas steps 3 + 4 ('oxidisable' and 'residual') indicated long-term immobilisation (these metals could only be extracted using harsh agents and may correspond to organic matter and/or aluminosilicates; compare Table 3, supplementary information). Therefore, the amounts extracted in steps 1 + 2 and 3 + 4 are added and the difference in the sum is considered to be the difference in long-term mobilisation potential (Δ_{mob}).

2.6. Solid-state speciation by XANES

Pb L_{III}-edge XANES experiments were performed at the superXAS beamline (Swiss Light Source, Villigen, Switzerland). Measurement details including sample preparation can be found in Section S5 of the Supporting Information.

2.7. Thermodynamic equilibrium modelling

Thermodynamic equilibrium modelling was performed using Geochemist's workbench software (Version 12.0) and the MINTEQ database (Gustafsson, 2014). The approach was used to create Pourbaix diagrams (electron activity (Eh) vs. pH) of the respective microcosm systems. The Pb^{2+} activity was based on the spiked concentration of the species in the system. The model took into account four main system components: i) rainwater composition (see Section 2.2), ii) main mineral-forming elements (Fe, Mn) after quantification via microwave-assisted acid digestion (Table S1, Supporting Information), iii) main anions typically present in soils (carbonate, phosphate) and iv) lactate for lactate-amended microcosms (Table S4, Supporting Information).

3. Results

3.1. Removal of Pb from the aqueous phase

Rapid and efficient removal of Pb from the perovskite (methylammonium lead triiodide (MAPI) and caesium-formamidinium lead triiodide (CsFAPI)) and $Pb(NO_3)_2$ species spiked in the soil-water systems from the aqueous phase under all of the tested conditions was observed (Fig. 1).

The dissipation half-lives of Pb in the system were short and all below 1 h (maximum of $t_{50\%}$= 0.86 h for MAPI under anaerobic conditions, Table S2, Supporting Information). In the first four hours, $Pb(NO_3)_2$ species showed a somewhat faster aqueous removal, while perovskite-derived species lagged behind (compare squares in Fig. 1 versus others). Hence, the times for a more complete aqueous removal were also higher for perovskite-derived species, but did not exceed 3.7 h ($t_{75\%}$) and 16.7 h ($t_{90\%}$) under all conditions tested (Table S2, Supporting Information). The application of different biogeochemical conditions did not lead to considerable differences in aqueous removal efficiency: after 24 h, the residual dissolved Pb concentration was low and total removal efficiency from the aqueous phase ranged between 92% and 98%, irrespective of the Pb source used.

3.2. Foreseen availability of Pb in soil

A large proportion of spiked Pb (48.0–62.8%) was extracted in oxidisable and residual fractions, irrespective of the spiked Pb species or the conditions applied (Fig. 2a–c, blue bars).

In $Pb(NO_3)_2$-spiked microcosms, a majority of Pb was found in fractions insusceptible to long-term mobilisation (i.e. 'oxidisable' and 'residual'), indicated by the strongly negative Δ_{mob} (Fig. 2c). In contrast, perovskite-derived Pb exhibited a higher tendency for long-term mobilisation (i.e. less negative Δ_{mob}) with one exception (MAPI in lactate-amended microcosms). In all cases, the exchangeable fraction was low (3.7 – 8.1%). Foreseen availability following short-term (48 h) exposure to soil was also investigated and no considerable difference in fractionation was observed (Fig. S2, Supporting Information).

3.3. Modelled Pb speciation

Pourbaix diagrams obtained from the thermodynamic modelling of the microcosm system pointed to the formation of insoluble Pb species under the tested conditions (Fig. 3a-b).

Under aerobic conditions (region 1 in Fig. 3a-b), mixed-metal phosphate phases, such as plumbgummite ($PbAl_3(PO_4)_2(OH)_5 \cdot H_2O$) (Fig. 3a) and hinsdalite ($(Pb,Sr)Al_3(PO_4)(SO_4)(OH)_6$) (data not shown), were the ultimate thermodynamic sinks for Pb^{2+}. Although thermodynamically favoured, these minerals rarely occur in nature (e.g., in oxidised zones of lead-bearing deposits (Kolitsch et al., 1999)). Therefore, these minerals were excluded from modelling, yielding more common (hydroxy)pyromorphite ($Pb_5(PO_4)_3(Cl,OH)$) as the favoured species instead (Fig. 3b). Upon Eh decrease toward more reducing conditions in lactate-amended microcosms (region 3, Fig. 3b), the (microbial) reduction of sulphate to sulphide became thermodynamically favoured; hence, the formation of highly insoluble galena (PbS) is preferred.

3.4. Determined solid-phase speciation

Soil microcosm samples were measured by XANES to determine Pb speciation. The absence of pronounced features in the XANES region between 13′050 and 13′100 eV indicated that Pb was not present as a (crystalline) precipitate similar to the reference samples tested (Fig. 4a).

For all of the tested soil samples, one or two-component models yielded accurate fits (as indicated by low residuals in Fig. 4b–d (dotted lines)). The addition of a third component led to an only marginally improved goodness-of-fit in some cases (see Table S5, Supporting Information). Linear Combination Fitting (LCF) analysis indicated that the highest share of Pb (63–100%) resembled a form similar to the Pb sorbed on birnessite (MnO_2) in all samples (Table 1). Smaller contributions of galena (PbS) and hydroxypyromorphite ($Pb_5(PO_4)_3(Cl,OH)$) (9–21%) were obtained regardless of spiked Pb species or applied biogeochemical conditions.

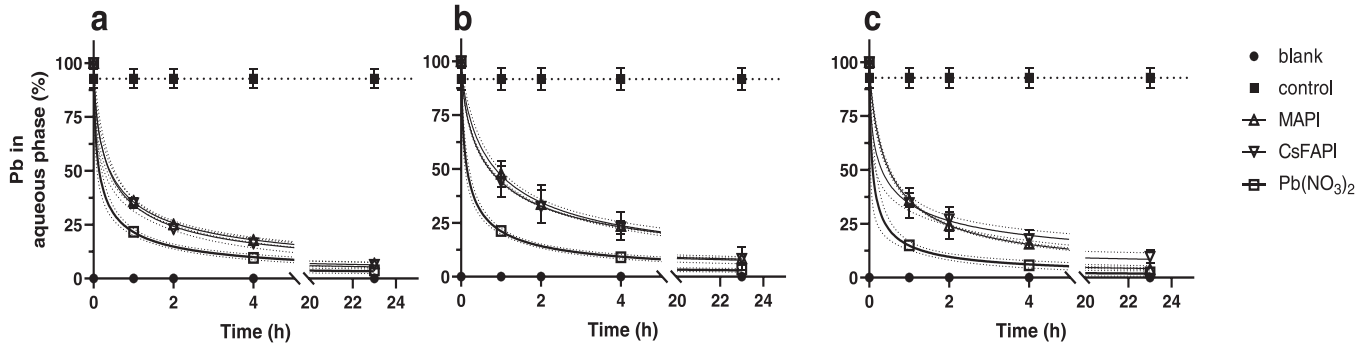

Fig. 1. Pb aqueous concentrations over time for different Pb sources under aerobic (a), anaerobic (b) and lactate amended (c) conditions. Non-linear regression was based on mean concentrations of triplicate measurements (dotted lines mark the 95% confidence intervals of the fits). Regression parameters and characteristic removal times and detailed in Table S2, Supporting Information.

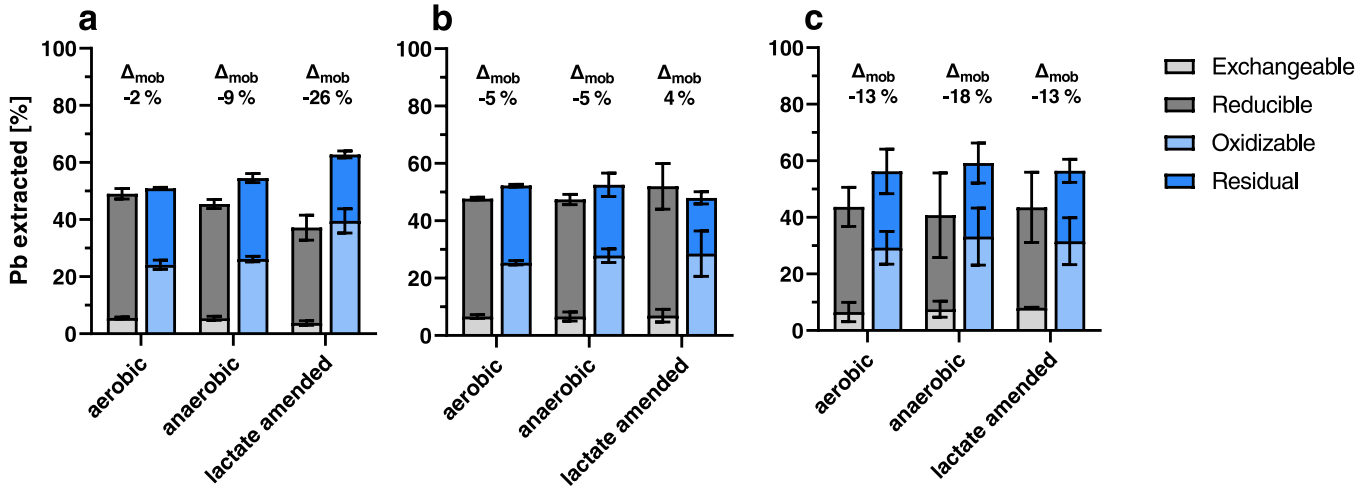

Fig. 2. Soil Pb fractionation after 16 d in microcosms spiked with (a) MAPI, (b) CsFAPI and (c) $Pb(NO_3)_2$. The first two sequential extraction steps (exchangeable + reducible) are prone to short and/or medium term mobilisation and are distinguished from the last two steps (oxidisable + residual) with Δ_{mob} relating to the difference in the sums. Error bars indicate standard deviations of triplicates.

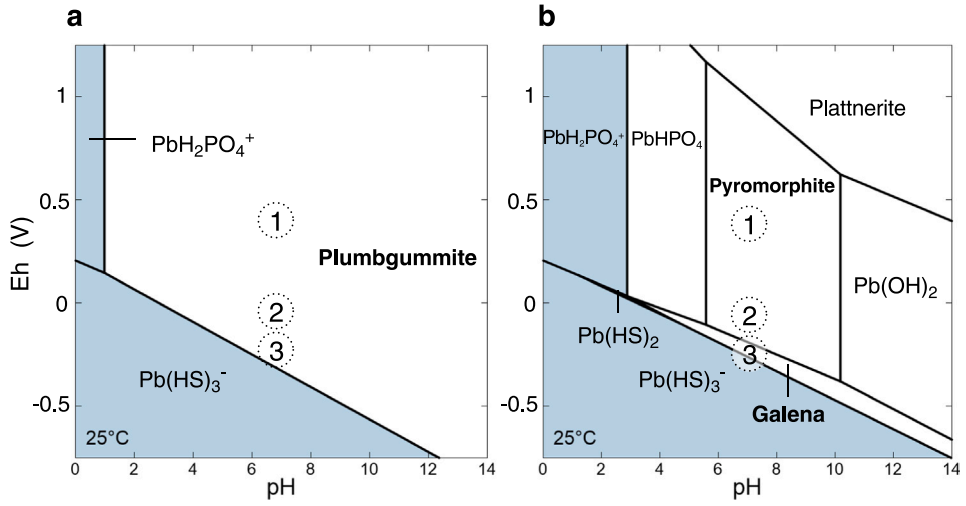

Fig. 3. Pourbaix diagrams of the thermodynamically favoured Pb species in microcosms (input parameters see Table S3, Supporting Information) with (a) full set of species and (b) plumbgummite and hinsdalite suppression. Blue regions refer to aqueous species, while white regions represent insoluble mineral phases. The dashed circles indicate the pH/Eh conditions measured in aerobic (1), anaerobic (2) and lactate amended (3) microcosms.

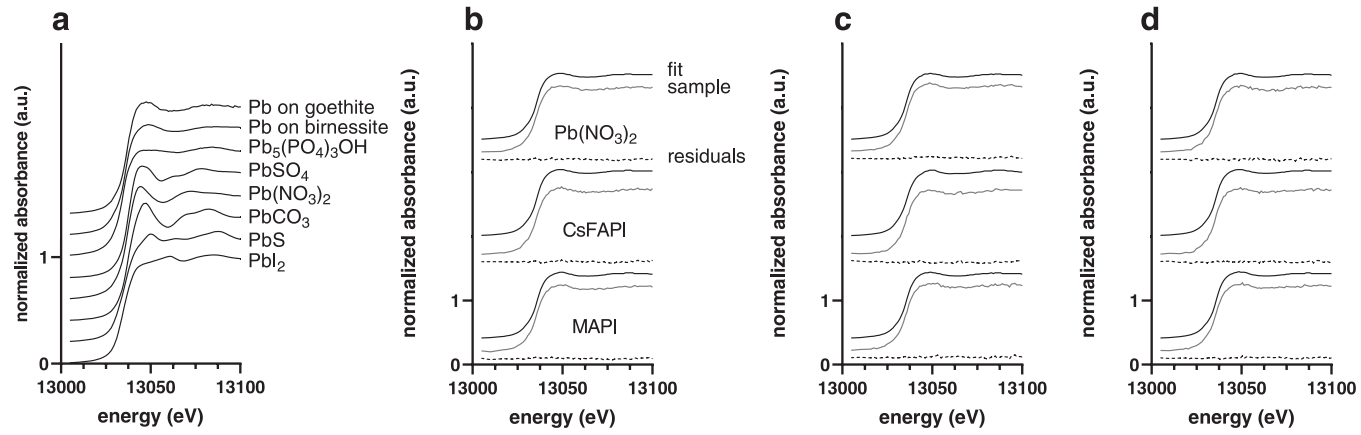

Fig. 4. Normalised Pb L_{III}-edge XANES spectra for reference compounds (a), aerobic (b), anaerobic (c) and lactate-amended microcosms (d). Microcosm experimental Pb XANES spectra of the different Pb sources ($Pb(NO_3)_2$ on top (b–d); CsFAPI in the middle; MAPI on bottom) are shown as solid lines; their best linear combination fits as grey lines and residuals as dashed lines (spectra are shifted in Y to improve readability).

Table 1
Pb speciation modelled by linear combination fitting of Pb L_{III}-Edge XANES Spectra with R-factor (measure for the mean square sum of the misfit) and χ^2 (goodness of fit). For details, refer to Section S5, Supporting Information.

Pb species	Contribution (atom %)				R factor	χ^2
	Condition	"Pb on birnessite"	Galena (PbS)	Hydroxypyromorphite ($Pb_5(PO_4)_3OH$)		
MAPI	Aerobic	87	13	–	0.00079	0.01445
	Anaerobic	81	–	19	0.00088	0.01577
	Lactate amended	100	–	–	0.00056	0.01073
CsFAPI	Aerobic	91	–	9	0.00048	0.00884
	Anaerobic	63	35	–	0.00164	0.03089
	Lactate amended	91	–	9	0.00051	0.00953
$Pb(NO_3)_2$	Aerobic	88	–	12	0.00036	0.00664
	Anaerobic	79	–	21	0.00274	0.05258
	Lactate amended	90	10	–	0.00074	0.01362

4. Discussion

4.1. Extent of aqueous Pb removal and kinetics

In all conditions tested here, a rapid ($t_{50\%} < 1$ h) removal of Pb from the aqueous phase was observed (Fig. 1a–c). This was true for all Pb sources used and observed despite the applied worst-case scenario, where a high concentration of Pb was immediately released to the soil. The experiments covered oxidising to strongly reducing redox conditions; thus, they were representative of many environments. The fact that the observed kinetics were similar in all conditions indicated that Pb removal from the aqueous phase was mainly driven by similar physical and not biological processes during initial (< 24 h) exposure. Comparing the spiked Pb species showed that, irrespective of the applied conditions, the kinetics of aqueous $Pb(NO_3)_2$ removal were somewhat faster as compared to those of both MAPI and CsFAPI (Table S2, $t_{50\%}$, $t_{75\%}$ and $t_{90\%}$, Supporting Information), yet the maximum time needed for the dissipation of 90% of Pb was only 16.7 h (Table S2, $t_{90\%}$, Supporting Information). The presence of additional cations (such as MA^+, Cs^+, FA^+) could result in additional competitive sorption, slowing down perovskite-derived Pb sorption kinetics. Although slight differences in kinetics occurred during the first hours of the experiment, the complete removal of Pb after 24 h in all approaches suggests that Pb from perovkites will not show a dramatically different transport behaviour in the environment compared to cationic lead.

The efficient sequestration observed here is in line with a previous study investigating sequestration of Pb derived from PbI_2 and PbO (Yoo et al., 2019). However, the applied concentrations previously were much higher, exceeding the solubility products of PbI_2 and PbO in an aqueous solution. As a consequence, the derived partitioning coefficients were probably too optimistic due to precipitation (and thus the proposed 'safety management areas per units of PSC power-plant output' in the original study possibly underestimated). Even though the Pb concentrations used here were lower by an order of magnitude, the soil still demonstrated a high potential for rapid and efficient Pb sequestration, which is positive in terms of the environmental risk associated with perovskite photovoltaics (see below).

4.2. Foreseen Pb availability and mechanism of Pb soil sequestration

Following the rapid and efficient removal from the aqueous phase, only minor amounts of Pb (maximum of 8.1%) were found in the environmentally most problematic fraction as 'exchangeable' Pb (i.e., step 1 of the sequential extraction; Table S3, Supporting Information). The exchangeable fraction was assessed by the addition of a weak organic acid, as a number of natural and anthropogenic processes moderately acidify soils (e.g. soil respiration, microbial nitrification or sulphide oxidation, microbial and plant exudate production, incineration of carbon-, nitrogen- and sulphur-containing compounds) (Zheng et al., 2012; Panthi et al.,). As a result, Pb released by weak acid addition can be re-mobilised immediately and may be considered available for plant uptake. Indeed, Li et al. have reported that the bioavailability of Pb from perovskite to various plants is greater than that of pure lead iodide over a 20-day exposure time (Li et al., 2020), which they attributed to organic cations (such as methylammonium and formamidinium) influencing soil pH. However, the absolute amounts of Pb spiked were rather high: using the assumptions of Li et al., infiltration area of 1 m^2 per m^2 of PV; soil depth affected 15 cm), the worst case scenario considered here would increase soil concentration by + 4 ppm only, whereas the authors have spiked between 5 and 250 ppm of Pb. In other words, to achieve

such an increase in Pb concentration, one would need to increase assumed perovskite layer thickness orders of magnitude above what is actually used (here 600 nm was assumed). Thus, the scenario may be rather relevant for a MAPI spill during production than leaching during the use phase. Due to the possible effect of competing cations on the sorption kinetic and the risk of exceeding solubility products (see above), this study underlines that risk assessment scenarios must be made with care to derive claims not under- or overstating possible adverse effects of perovskite derived Pb in the environment.

Further, it should be noted that plant growth experiments on freshly spiked soils (as performed by Li et al., 2020) are known lead to discrepancies compared to field studies in terms of plant availability due to ageing (Udovic and Lestan, 2009; Liu et al., 2016). Ageing over long time periods (such as decades) is known to influence speciation and thus availability compared to spiked metals (Antoniadis et al., 2017). Here, 16 days of contact resulted in somewhat higher Pb immobilisation (i.e. more negative Δ_{mob}; compare Fig. 2 and Fig. S2) compared to 2 days in aerobic conditions, which are possibly most similar to Li et al. (2020). Thus, it remains to be elucidated, if perovskite-derived Pb is indeed more plant-available during a regular growth season outdoors. In particular, one should consider scenarios where Pb enters the pedosphere before plants start to grow (giving the possibility for ageing), at a low concentration of Pb (not exceeding solubility limits and being in line with how much Pb can actually leach from a PV module). In terms of the exchangeable fraction representing readily plant-available Pb (at low Pb spiking, without extended ageing), our data suggests that there will be little to no differences.

In addition to the exchangeable fraction, Pb found in the 'reducible fraction' (i.e. step 2, Table S3, Supporting Information) may be prone to become mobilised and available in the medium term (indicative timescale weeks to months). With the depletion of oxygen, the reduction of different mineral phases becomes thermodynamically favoured and their – to a large extent microbially-driven – dissolution releases metals into the soil solution (Borch et al., 2010). In fact, owing to oscillations between oxidising and reducing conditions, mineral dissolution and formation are common in soils (e.g. during water logging, periodic flooding and between dry and wet seasons), leading to a coloration that is characteristic for such oscillations (so-called 'redoximorphic features') (Gasparatos, 2012). Induction of reducing conditions has been reported to lead to the mobilisation of the associated Pb (Hernandez-Soriano and Jimenez-Lopez, 2012; de Campos et al., 2020). In contrast, Pb associated to the 'oxidisable' and 'reducible' fraction (Table S3, Supporting Information) will only be released in geological time scales upon mineral weathering and can be considered stably sequestered and not available (Sungur et al., 2014; Janoš et al., 2010; Ashrafi et al., 2015). $Pb(NO_3)_2$ showed a slightly higher extent of stably sequestered Pb (indicated by the lower Δ_{mob}, Fig. 2) in comparison to MAPI- and CsFAPI-derived Pb. Considering that ageing of metals may continue far longer than the 16 days tested here and that microcosms with microbial activity stimulated by lactate addition had the lowest Δ_{mob} of all conditions tested using MAPI (Fig. 2A) it is questionable, if this is really relevant for environmental risk assessment. The considerably higher Δ_{mob} in the corresponding CsFAPI experiments (Fig. 2B) leaves room for some speculation of the effect of the organic cation. While simple methyl compounds (such as di- and trimethylamine) are a direct substrate for methanogens (Thauer et al., 2008) and fully mineralised to methane, CO_2 and ammonium, it can be doubted that the C=N bond in the formamidinium cation is as easy to cleave (C=N bond energy > 600 kJ/mol). Thus, the formamidinium cation may tentatively persist and continue to compete for sorption and/or reactive sites in soil, resulting in higher Δ_{mob} in CsFAPI experiments.

Sequential extraction is known to have some limitations related to selectivity (Bacon and Davidson, 2008; Calmano et al., 2001) and cannot provide information on the underlying sequestration mechanism. Thermodynamic modelling revealed precipitation as a potential mechanism of Pb^{2+} sequestration, mainly in phosphatic mineral phases (aerobic conditions; region 1 in Fig. 3) and galena (PbS) (anaerobic conditions; regions 2 and 3 in Fig. 3). This would suggest very low aqueous Pb concentrations due to the low solubility products of these mineral phases. XANES spectra on the Pb L_{III}-edge of the microcosms were clearly dissimilar to a number of solid references used (i.e. $PbSO_4$, $Pb(NO_3)_2$; $PbCO_3$, PbS, or PbI_2) that had prominent features in the range ~13′050–13′100 eV (Fig. 4). Indeed, LCF yielded best fits with the major contribution of the reference 'Pb on birnessite' (63–100%, Table 1) and only minor contributions (between 0% and 21%) of possible precipitates (i.e. hydroxypyromorphite ($(Pb_5(PO_4)_3(Cl,OH)$) and galena (PbS); Table 1). The XANES spectra of two references of sorbed species used here (i.e. 'Pb on birnessite', 'Pb on goethite') were similar to each other and similar with those of other sorbed species found in literature (see e.g. Nevidomskaya et al., 2016; Smith et al., 2011). As a consequence, the actual sorbing phase could not be resolved through XANES at the Pb concentrations applied here. In fact, Pb may be even sorbed to several phases at once, including organic matter or aluminosilicates (such as bentonite, kaolinite, and gibbsite), all yielding similar XANES spectra (Nevidomskaya et al., 2016; Smith et al., 2011). This may explain why Pb was found in the 'reducible' as well as 'oxidisable' and 'residual' fractions at once (Fig. 2). Whereas some Pb may indeed sorb to manganese phases (that are extracted in the 'reducible' fraction), (Kwon et al., 2010; Lee et al., 2011) aluminosilicates would not dissolve during the mild treatment of the first two steps of the sequential extraction and rather require harsher conditions (as in steps three and four). Despite the fact that the sorbing phase could not be resolved by XANES analysis, the precipitation of hydroxypyromorphite ($Pb_5(PO_4)_3(Cl,OH)$) and galena (PbS) (predicted by thermodynamic modelling) gave only a minor contribution to the best fits; thus, their precipitation was apparently kinetically limited.

4.3. Environmental implications

Two major worst-case scenarios, a solar park and a rooftop installation of perovskites, were considered to assess the environmental implications of the sequestration phenomena observed here. First, in a 'solar park-type' installation, one may assume that rain leaches a damaged module and that Pb enters the soil below the module by dripping water (Fig. S3, Supporting Information). In the worst-case scenario, the module would be fully damaged so that all Pb leaches of a typical PSC module (1.64 m × 1 m) into a narrow soil fragment (e.g., 10 cm) along the module width. Based on a given soil density (e.g., 1′500 kg/m^3) and depth (e.g., 2.5 cm for topsoil), the Pb concentration will increase to 112 mg/kg (see Section S2 for details). This is in line with some early estimations reported by Hailegnaw et al. (2015) using non-encapsulated perovskite films and possibly overestimating the actual Pb input to the pedosphere. Nevertheless, our data shows the majority (> 90%) of Pb was removed from the aqueous phase in less than a day which limits Pb dispersal, and that only 37 – 52% of spiked Pb could potentially be liberated (in the medium term under induction of reducing conditions). Thus, even if all Pb leaches from the module, the potentially bioavailable Pb fraction corresponds to 41.1–58.2 mg/kg, only. Considering common soil Pb background concentrations in the range of 50 mg/kg (Alfaro et al., 2015), this can be considered a very moderate impact even in the worst-case. Considering that the exchangeable fractions corresponded to possibly plant-available Pb, the additional Pb concentration amounted to only 4.3–9.1 mg/kg. Putting this into the perspective of toxicity to soil organisms (e.g. *Folsomia candida* (springtail): LC_{50} = 2′562 mg/kg and EC_{50} (reproduction) = 1′244 mg/kg (Dai et al., 2020) or *Eisenia fetida* (earth worm): EC_{50} (reproduction) = 35–5′080 mg/kg (Lanno et al., 2019)), again impacts can be considered marginal. Finally, the European Chemicals Agency mentions a "predicted no effect concentration" (PNEC) for Pb in soil of 212 mg/kg, which implies no adverse effects whatsoever on soil biota. Some safety concerns based on lead uptake from plants for human consumption have been raised by Li et al. recently (Li et al., 2020). First,

it can be doubted that plant for human consumption are grown on a perovskite solar park. Secondly, it should be noted, that for this exposure pathway Pb transfer to edible parts is of importance (rather than stem- or root-associated Pb). At low Pb levels that are more realistic to occur in a solar park (e.g. 5 mg/kg), Pb concentration in leaves increased marginally, while PbI_2 experiments showed lower Pb levels relative to controls, questioning the efficient transfer of Pb to edible parts at relevant concentrations. Bioavailability studies are certainly indispensable when assessing impacts of metals. However, more research is required to unequivocally prove higher bioavailability from perovskite-derived Pb in the field.

Second, in a 'rooftop' scenario, one may consider that Pb is completely released from a module (same as above) within a single rain event (e.g., 100 L/m^2 as a one-day maximum in Switzerland). Again, this is a worst-case scenario and it seems likely that not all perovskite film is exposed to rain and thus leaching. It can be assumed that leached Pb would be collected using a downpipe before it is collected for re-use, percolated in a soaking area or directed to the sewer system. In the downpipe, aqueous Pb concentrations can be elevated in absence of a sorbing phase. For example, assuming quantitative Pb leaching from a 80 m^2 PSC-covered roof in a single 100 mm rain event would result in a Pb concentration in the effluent of 4.2 mg/L in the downpipe itself. Although diluted in the rainwater barrel or tank, it is certainly not advisable to re-use the collected rain after such an event but rather treat it (e.g. by ion exchange resins or other methods).

If the rainwater is not re-used but directly percolated, the Pb soil concentration increase can be calculated similarly as for the solar park scenario, but possibly on a larger area. For instance, given a soaking area of 16 m^2 (in domestic applications), Pb concentrations in the top 2.5 cm of soil at the bottom of the soaking area, would increase by 56 mg/kg, assuming there is no sorption to the percolation filling material itself. Compared to the increase from the solar park scenario, this Pb concentration is halved and the bioavailable Pb fractions would be even lower. Thus, percolation on a larger area would ease the concerns of Pb impacts.

To our best knowledge, the concentration of Pb that may enter the sewer system from domestic rooftops is not yet clearly regulated. Obviously, the drinking water limit of 5 μg/L (EU Drinking Water Directive) is too restrictive. Rather one can assume the limit of 200 μg/L, which applies to industrial effluents (EU Industrial Emissions Directive). Hence, assuming a concentration of 4.6 mg/L in the downpipe would require a dilution by factor 23, which is high considering 80 m^2 of perovskite covered roof area. Again, this suggests that in the highly unlikely case that all perovskite Pb leaches in a single rain event, the rain should rather be collected in a buffer tank and treated rather than directly fed into the sewer.

These considerations underline the importance of exposure pathways when assessing the risk associated to perovskite photovoltaics. From the data gathered here, no concerns are raised as long as there is a potent sorbing phase, such as a soil, present that dissipates aqueous Pb and decreases the bioavailable fraction.

5. Conclusions

High-efficiency perovskite solar cells critically depend on Pb-based absorber materials. In this study, soil was shown to be a potent natural matrix for the stable sequestration of a majority of Pb possibly released from damaged modules. Dissipation half-lives of Pb in the aqueous phase were less than 1 h, and only a marginal fraction of Pb in soil (< 8%) was found to be readily mobile and/or bioavailable. However, sorption to reducible mineral phases such as Fe(III)- or Mn(IV)-oxides may result in partial re-mobilisation of the Pb previously sequestered. This is expected in the medium term when reducing conditions develop upon water logging or flooding, leaving some time for remediation intervention (e.g., excavating the top few cm of soil). Since electricity production is only possible having an intact perovskite layer, such interventions should be considered as soon as module failure is detected, if inspection reveals loss of lead. Although the sorption kinetics and extractable Pb were slightly different, the data from this study do not suggest that perovskites derived Pb will differ greatly in environmental fate from cationic lead. Ultimately, however, further trials (well-designed field trials including ecotoxicity) are needed to draw a definitive conclusion.

Environmental Implications

Novel solar cells based on perovskite-based absorber materials are considered a potential breakthrough technology for green energy generation. However, high-efficiency perovskite solar cells rely on the use of cationic Pb, which is of environmental concern i) during fabrication, ii) in case of damage and iii) at the end of life. Here, we present novel insights into the fate these potentially hazardous, perovskite-derived Pb under realistic environmental conditions in soil-water microcosms. Our results indicate that the fate of perovskite-derived Pb species is in fact similar compared to cationic Pb implying that previous risk assessment considerations still remain valid.

Author contributions

M.L. and F.S. conceptualised the study. F.S. carried out all experimental and modelling work. L.L. assisted in the experimental setup. M. L., H.J.S. and A.S. supervised the work. All authors have given approval to the final version of the manuscript.

Funding sources

This project has received funding from the European Union's Horizon 2020 Framework Program for research and innovation under grant agreement no 763977 of the PerTPV project.

CRediT authorship contribution statement

Felix Schmidt: Methodology, Investigation, Writing – original draft, Writing – review & editing, Visualization. **Luca Ledermann:** Investigation. **Andreas Schäffer:** Writing – review & editing, Supervision. **Henry J. Snaith:** Writing – review & editing, Supervision, Funding acquisition. **Markus Lenz:** Conceptualization, Methodology, Writing – review & editing, Visualization, Supervision, Funding acquisition

Declaration of Competing Interest

The authors declare that they have no known competing financial interests or personal relationships that could have appeared to influence the work reported in this paper.

Acknowledgements

We thank Maarten Nachtegaal and Adam H. Clark for help during XAS measurements and for helpful comments on the manuscript.

Appendix A. Supporting information

The following files are available free of charge:
Document 1:

1. Soil Characterisation
   - o Table S1: Soil characterisation after MW digestion
2. Kinetics of aqueous Pb removal
   - o Table S2: Aqueous Pb removal times and fits
3. Sequential Extraction
   - o Table S3: Sequential extraction conditions
   - o Fig. S1: Sequential extraction validation results

- o Fig. S2: Short-term sequestration
4. Thermodynamic modelling
   - o Table S4: Thermodynamic modelling input
5. XANES measurements
   - o Table S5: Three component LCF and comparison of goodness of fit parameters with two-component LCF.
6. Assumptions for predicted environmental concentrations
   - o Fig. S3: Scheme for solar park scenario

Appendix B. Supporting information

Supplementary data associated with this article can be found in the online version at doi:10.1016/j.jhazmat.2022.128995.

References

Alfaro, M.R., Montero, A., Ugarte, O.M., do Nascimento, C.W.A., de Aguiar Accioly, A.M., Biondi, C.M., da Silva, Y.J.A.B., 2015. Background concentrations and reference values for heavy metals in soils of Cuba. Environ. Monit. Assess. 187, 1–10.

Antoniadis, V., Levizou, E., Shaheen, S.M., Ok, Y.S., Sebastian, A., Baum, C., Prasad, M.N. V., Wenzel, W.W., Rinklebe, J., 2017. Trace elements in the soil-plant interface: phytoavailability, translocation, and phytoremediation–a review. Earth-Sci. Rev. 171, 621–645.

Arain, M.B., Kazi, T.G., Jamali, M.K., Jalbani, N., Afridi, H.I., Baig, J.A., 2008. Speciation of heavy metals in sediment by conventional, ultrasound and microwave assisted single extraction methods: a comparison with modified sequential extraction procedure. J. Hazard. Mater. 154, 998–1006.

Ashrafi, M., Mohamad, S., Yusoff, I., Hamid, F.S., 2015. Immobilization of Pb, Cd, and Zn in a contaminated soil using eggshell and banana stem amendments: metal leachability and a sequential extraction study. Environ. Sci. Pollut. Res. 22, 223–230.

Ata, S., Tabassum, A., Bibi, I., Majid, F., Sultan, M., Ghafoor, S., Bhatti, M.A., Qureshi, N., Iqbal, M., 2019. Lead remediation using smart materials. A review. Z. Für Phys. Chem. 233, 1377–1409.

Babayigit, A., Ethirajan, A., Muller, M., Conings, B., 2016. Toxicity of organometal halide perovskite solar cells. Nat. Mater. 15, 247–251.

Bacon, J.R., Davidson, C.M., 2008. Is there a future for sequential chemical extraction? Analyst 133, 25–46.

Bell, W.B., 1924. Influence of lead on normal and abnormal cell growth and on certain organs. Lancet 1, 267–276.

Bellinger, D.C., 2016. Lead contamination in Flint—an abject failure to protect public health. New Engl. J. Med. 374, 1101–1103.

Borch, T., Kretzschmar, R., Kappler, A., Van Cappellen, P., Ginder-Vogel, M., Voegelin, A., Campbell, K., 2010. Biogeochemical redox processes and their impact on contaminant dynamics. Environ. Sci. Technol. 44, 15–23.

Calmano, W., Mangold, S., Welter, E., 2001. An XAFS investigation of the artefacts caused by sequential extraction analyses of Pb-contaminated soils, Fresenius'. J. Anal. Chem. 371, 823–830.

de Campos, A.K.R., Cavalieri-Polizeli, K.M.V., 2020. Effects of compaction on lead availability in contaminated soils with contrasting texture. Environ. Monit. Assess. 192, 1–12.

Case, C., Beaumont, N., Kirk, D., 2019. Industrial insights into Perovskite Photovoltaics. ACS Energy Lett. 4, 2760–2762.

Celik, I., Song, Z., Cimaroli, A.J., Yan, Y., Heben, M.J., Apul, D., 2016. Life Cycle Assessment (LCA) of perovskite PV cells projected from lab to fab. Sol. Energy Mater. Sol. Cells 156, 157–169.

Chaney, R.L., Mielke, H.W., Sterrett, S.B., 1989. Speciation, mobility and bioavailability of soil lead. Environ. Geochem. Heal. 11, 105–129.

Dai, W., Holmstrup, M., Slotsbo, S., Ke, X., Li, Z., Gao, M., Wu, L., 2020. Compartmentation and effects of lead (Pb) in the collembolan, Folsomia candida. Environ. Sci. Pollut. Res. 27, 43638–43645.

Diau, E.W.-G., Jokar, E., Rameez, M., 2019. Strategies to improve performance and stability for tin-based perovskite solar cells. ACS Energy Lett. 4, 1930–1937.

Espinosa, N., Serrano-Luján, L., Urbina, A., Krebs, F.C., 2015. Solution and vapour deposited lead perovskite solar cells: Ecotoxicity from a life cycle assessment perspective. Sol. Energy Mater. Sol. Cells 137, 303–310.

Evangelou, M.W.H., Brem, A., Ugolini, F., Abiven, S., Schulin, R., 2014. Soil application of biochar produced from biomass grown on trace element contaminated land. J. Environ. Manag. 146, 100–106.

Fabini, D., 2015. Quantifying the potential for lead pollution from halide perovskite photovoltaics. J. Phys. Chem. Lett. 6, 3546–3548.

Fthenakis, V., Athias, C., Blumenthal, A., Kulur, A., Magliozzo, J., Ng, D., 2020. Sustainability evaluation of CdTe PV: An update. Renew. Sustain. Energy Rev. 123, 109776.

Gasparatos, D., 2012. Fe–Mn concretions and nodules to sequester heavy metals in soils. Environ. Chem. A Sustain. World 443–474.

Grätzel, M., 2017. The rise of highly efficient and stable perovskite solar cells. Acc. Chem. Res. 50, 487–491.

Green, M.A., Dunlop, E.D., Levi, D.H., Hohl-Ebinger, J., Yoshita, M., Ho-Baillie, A.W.Y., 2019. Solar cell efficiency tables (version 54). Prog. Photovolt. Res. Appl. 27, 565–575.

J.P. Gustafsson, Visual MINTEQ 3.1, Sweden, Stock. (KTH R. Inst. Technol. Dep. L. Water Resour. Eng. , 2014).

Habisreutinger, S.N., McMeekin, D.P., Snaith, H.J., Nicholas, R.J., 2016. Research Update: Strategies for improving the stability of perovskite solar cells. APL Mater. 4, 91503.

Hailegnaw, B., Kirmayer, S., Edri, E., Hodes, G., Cahen, D., 2015. Rain on methylammonium lead iodide based perovskites: Possible environmental effects of perovskite solar cells. J. Phys. Chem. Lett. 6, 1543–1547.

Hernandez-Soriano, M.C., Jimenez-Lopez, J.C., 2012. Effects of soil water content and organic matter addition on the speciation and bioavailability of heavy metals. Sci. Total Environ. 423, 55–61.

Janoš, P., Vávrová, J., Herzogová, L., Pilavrová, V., 2010. Effects of inorganic and organic amendments on the mobility (leachability) of heavy metals in contaminated soil: a sequential extraction study. Geoderma 159, 335–341.

Jokar, E., Chien, C.-H., Tsai, C.-M., Fathi, A., Diau, E.W.-G., 2019. Robust tin-based perovskite solar cells with hybrid organic cations to attain efficiency approaching 10%. Adv. Mater. 31, 1804835.

Kamat, P.V., Bisquert, J., Buriak, J., 2017. Lead-free perovskite solar cells. ACS Energy Lett. 2, 904–905.

Ke, W., Kanatzidis, M.G., 2019. Prospects for low-toxicity lead-free perovskite solar cells. Nat. Commun. 10, 965.

Kojima, A., Teshima, K., Shirai, Y., Miyasaka, T., 2009. Organometal halide perovskites as visible-light sensitizers for photovoltaic cells. J. Am. Chem. Soc. 131, 6050–6051.

Kolitsch, U., Tiekink, E.R.T., Slade, P.G., Taylor, M.R., Pring, A., 1999. Hinsdalite and plumbogummite, their atomic arrangements and disordered lead sites. Eur. J. Mineral. 513–520.

Kwon, K.D., Refson, K., Sposito, G., 2010. Surface complexation of Pb (II) by hexagonal birnessite nanoparticles. Geochim. Cosmochim. Acta 74, 6731–6740.

Lanno, R.P., Oorts, K., Smolders, E., Albanese, K., Chowdhury, M.J., 2019. Effects of soil properties on the toxicity and bioaccumulation of lead in soil invertebrates. Environ. Toxicol. Chem. 38, 1486–1494.

Lee, M.M., Teuscher, J., Miyasaka, T., Murakami, T.N., Snaith, H.J., 2012. Efficient hybrid solar cells based on meso-superstructured organometal halide perovskites. Science 338, 643–647. https://doi.org/10.1126/science.1228604.

Lee, S., An, J., Kim, Y.-J., Nam, K., 2011. Binding strength-associated toxicity reduction by birnessite and hydroxyapatite in Pb and Cd contaminated sediments. J. Hazard. Mater. 186, 2117–2122.

Li, J., Cao, H.-L., Jiao, W.-B., Wang, Q., Wei, M., Cantone, I., Lü, J., Abate, A., 2020. Biological impact of lead from halide perovskites reveals the risk of introducing a safe threshold. Nat. Commun. 11, 1–5.

Liu, W.-W., Wu, T.-H., Liu, M.-C., Niu, W.-J., Chueh, Y.-L., 2019. Recent challenges in perovskite solar cells toward enhanced stability, less toxicity, and large-area mass production. Adv. Mater. Interfaces 6, 1801758.

Liu, Z., Hamuti, A., Abdulla, H., Zhang, F., Mao, X., 2016. Accumulation of metallic elements by native species thriving in two mine tailings in Aletai, China. Environ. Earth Sci. 75, 781.

Nevidomskaya, D.G., Minkina, T.M., Soldatov, A.V., Shuvaeva, V.A., Zubavichus, Y.V., Podkovyrina, Y.S., 2016. Comprehensive study of Pb (II) speciation in soil by X-ray absorption spectroscopy (XANES and EXAFS) and sequential fractionation. J. Soils Sediment. 16, 1183–1192.

Nishimura, K., Kamarudin, M.A., Hirotani, D., Hamada, K., Shen, Q., Iikubo, S., Minemoto, T., Yoshino, K., Hayase, S., 2020. Lead-free tin-halide perovskite solar cells with 13% efficiency. Nano Energy, 104858.

G. Panthi, R. Bajagain, Y.-J. An, S.-W. Jeong, Leaching potential of chemical species from real perovskite and silicon solar cells, Process Saf. Environ. Prot. 149 (n.d.), pp. 115–122.

Quevauviller, P., 2002. Operationally-defined extraction procedures for soil and sediment analysis. Part 3: New CRMs for trace-element extractable contents. TrAC Trends Anal. Chem. 21, 774–785.

Rong, Y., Hu, Y., Mei, A., Tan, H., Saidaminov, M.I., Il Seok, S., McGehee, M.D., Sargent, E.H., Han, H., 2018. Challenges for commercializing perovskite solar cells. Science 361.

Smith, E., Kempson, I.M., Juhasz, A.L., Weber, J., Rofe, A., Gancarz, D., Naidu, R., McLaren, R.G., Gräfe, M., 2011. In vivo-in vitro and XANES spectroscopy assessments of lead bioavailability in contaminated periurban soils. Environ. Sci. Technol. 45, 6145–6152.

Smith, E.J., Davison, W., Hamilton-Taylor, J., 2002. Methods for preparing synthetic freshwaters. Water Res. 36, 1286–1296.

Sungur, A., Soylak, M., Ozcan, H., 2014. Investigation of heavy metal mobility and availability by the BCR sequential extraction procedure: relationship between soil properties and heavy metals availability. Chem. Speciat. Bioavailab. 26, 219–230.

Taylor, J.Y., Wright, M.L., Housman, D., 2016. Lead toxicity and genetics in Flint, MI, NPJ. Genom. Med. 1, 1–2.

Thauer, R.K., Kaster, A.-K., Seedorf, H., Buckel, W., Hedderich, R., 2008. Methanogenic archaea: ecologically relevant differences in energy conservation. Nat. Rev. Microbiol. 6, 579–591.

Udovic, M., Lestan, D., 2009. Pb, Zn and Cd mobility, availability and fractionation in aged soil remediated by EDTA leaching. Chemosphere 74, 1367–1373.

Urbina, A., 2020. The balance between efficiency, stability and environmental impacts in perovskite solar cells: a review. J. Phys. Energy 2, 22001.

Yoo, Y.G., Park, J., Umh, H.N., Lee, S.Y., Bae, S., Kim, Y.H., Jerng, S.E., Kim, Y., Yi, J., 2019. Evaluating the environmental impact of the lead species in perovskite solar cells via environmental-fate modeling. J. Ind. Eng. Chem. 70, 453–461.

Zheng, S., Zheng, X., Chen, C., 2012. Leaching behavior of heavy metals and transformation of their speciation in polluted soil receiving simulated acid rain. PLoS One 7, e49664.